Chem. Mater. **1993,** *5,* 720–725

ESR Study of the Formation of Superconducting Rb_3C_{60} from Solution

John A. Schlueter, H. Hau Wang,* Michael W. Lathrop, Urs Geiser,
K. Douglas Carlson, James D. Dudek, George A. Yaconi, and Jack M. Williams

*Chemistry and Materials Science Divisions, Argonne National Laboratory,
Argonne, Illinois 60439–4831*

Received December 22, 1992. Revised Manuscript Received March 9, 1993

A solution-based procedure, requiring reaction times less than 2 h, has been developed for the rapid preparation of Rb_3C_{60} (T_c onset = 29.0 ± 0.1 K) with superconducting shielding fractions near 50%. A 9:1 (vol) toluene/benzonitrile solvent system was used, which prevents premature precipitation of C_{60} as a monoanion. The Rb_xC_{60} material prepared in this manner from solution has been characterized by an ESR line-shape analysis at room temperature. In rigorously dried toluene, the primary product is RbC_{60}, but as the solvent polarity is increased with the addition of benzonitrile as a "redox catalyst", a greater fraction of superconducting Rb_3C_{60} is precipitated. The different room-temperature ESR line widths and integrated spin susceptibilities of these two products are used to quantify the relative yields of these two $C_{60}{}^{n-}$ species. The superconducting shielding fraction of the as formed "Rb_xC_{60}" product is found to correlate linearly with the Rb_3C_{60} content obtained from ESR line-shape analysis, confirming that Rb_3C_{60} is the only superconducting component prepared via this solution phase technique. ESR analysis revealed that Rb_3C_{60} samples (with shielding fractions near 100%) prepared by the conventional vapor phase technique contained a few percent RbC_{60}. X-ray powder diffraction confirmed the presence of trace amounts of RbCN in the solution-phase prepared materials.

Introduction

Samples of M_3C_{60} with superconducting shielding fractions near 100% have been obtained by combining C_{60} with stoichiometric amounts of alkali metals (M)[1–4] or M_6C_{60}[5] in sealed quartz reaction tubes followed by heat treatment at 200–250 °C for 10–15 days. The reaction initially involves the formation of M_6C_{60} on the fullerene grain surfaces.[2] Upon reductive doping, the tetrahedral and octahedral sites of the face centered cubic (fcc) C_{60} lattice are filled, with a fcc lattice being maintained for M_3C_{60} with $x \leq 3$.[6–9] C_{60} has also been doped with mixed alkali metals,[10–12] resulting in T_c's as high as 33 K in the mixed-metal compound Cs_2RbC_{60}.[13] With time, the alkali metal diffuses through the solid forming the desired M_3C_{60} salt. Samples prepared by this doping method generally require from several days to a few weeks of heat treatment and annealing.

A solution-phase preparation of M_3C_{60} is desirable for several reasons. Compared to the vapor-phase preparation, lower temperatures are required, reaction times should be substantially reduced, and the products formed should be more homogeneous. The phases formed from solution-based reactions have not been thoroughly investigated and controlled synthesis of the desired M_3C_{60} not perfected. Small superconducting shielding fractions, generally less than 7%, have been reported from solution-phase reactions.[14–16] Here we describe a much improved solution phase synthesis of Rb_3C_{60} involving reaction times of less than 2 h which results in superconducting shielding fractions in excess of 50%. ESR spectroscopy and X-ray powder diffraction have been used to quantify and characterize the various products formed by use of this procedure.

Experimental Section

Starting Materials. Toluene (Mallinckrodt AR) was freshly distilled from sodium under a nitrogen atmosphere prior to use.

---

(1) Hebard, A. F.; Rosseinsky, M. J.; Haddon, R. C.; Murphy, D. W.; Glarum, S. H.; Palstra, T. T. M.; Ramirez, A. P.; Kortan, A. R. *Nature* **1991**, *350*, 600–601.

(2) Holczer, K.; Klein, O.; Huang, S.-M.; Kaner, R. B.; Fu, K.-J.; Whetten, R. L.; Diederich, F. *Science* **1991**, *252*, 1154–1157.

(3) Zhou, O.; Fischer, J. E.; Coustel, N.; Kycia, S.; Zhu, Q.; McGhie, A. R.; Romanow, W. J.; McCauley, Jr., J. P.; Smith III, A. B.; Cox, D. E. *Nature* **1991**, *351*, 462–464.

(4) Zhang, Z.; Chen, C.-C.; Lieber, C. M. *Science* **1991**, *254*, 1619–1621.

(5) McCauley Jr., J. P.; Zhu, Q.; Coustel, N.; Zhou, O.; Vaughan, G.; Idziak, S. H. J.; Fischer, J. E.; Tozer, S. W.; Groski, D. M.; Bykovetz, N.; Lin, C. L.; McGhie, A. R.; Allen, B. H.; Romanow, W. J.; Denenstein, A. M.; Smith III, A. B. *J. Am. Chem. Soc.* **1991**, *113*, 8537–8538.

(6) Fischer, J. E.; Heiney, P. A.; Smith III, A. B. *Acc. Chem. Res.* **1992**, *25*, 112–118.

(7) Stephens, P.; Mihaly, L.; Lee, P. L.; Whetten, R. L.; Huang, S.-M.; Kaner, R.; Diederich, F.; Holczer, K. *Nature* **1991**, *351*, 632–634.

(8) Zhu, Q.; Zhou, O.; Coustel, N.; Vaughn, G. B. M.; McCauley Jr., J. P.; Romanow, W. J.; Fischer, J. E.; Smith III, A. B. *Science* **1991**, *254*, 545–548.

(9) Fleming, R. M.; Ramirez, A. P.; Rosseinsky, M. J.; Murphy, D. W.; Haddon, R. C.; Zahurak, S. M.; Makhija, A. V. *Nature* **1991**, *352*, 787–788.

(10) Tanigaki, K.; Hirosawa, I.; Ebbesen, T. W.; Mizuki, J.; Shimakawa, Y.; Kubo, Y.; Tsai, J. S.; Kuroshima, S. *Nature* **1992**, *356*, 419–421.

(11) Rosseinsky, M. J.; Murphy, D. W.; Fleming, R. M.; Tycko, R.; Ramirez, A. P.; Siegrist, T.; Dabbagh, G.; Barrett, S. E. *Nature* **1992**, *356*, 416–418.

(12) Chen, C.-C.; Kelty, S. P.; Lieber, C. M. *Science* **1991**, *253*, 886–888.

(13) Tanigaki, K.; Ebbesen, T. W.; Saito, S.; Mizuki, J.; Tsai, J. S.; Kubo, Y.; Kuroshima, S. *Nature* **1991**, *352*, 222–223.

(14) Wang, H. H.; Kini, A. M.; Savall, B. M.; Carlson, D. D.; Williams, J. M.; Lykke, K. R.; Wurz, P.; Parker, D. H.; Pellin, M. J.; Gruen, D. M.; Welp, U.; Kwok, W.-K.; Fleshler, S.; Crabtree, G. W. *Inorg. Chem.* **1991**, *30*, 2838–2839.

(15) Wang, H. H.; Kini, A. M.; Savall, B. M.; Carlson, K. D.; Williams, J. M.; Lathrop, M. W.; Lykke, K. R.; Parker, D. H.; Wurz, P.; Pellin, M. J.; Gruen, D. M.; Welp, U.; Kwok, W.-K.; Fleshler, S.; Crabtree, G. W.; Schirber, J. E.; Overmyer, D. L. *Inorg. Chem.* **1991**, *30*, 2962–2963.

(16) Murphy, D. W.; Rosseinsky, M. J.; Fleming, R. M.; Tycko, R.; Ramirez, A. P.; Haddon, R. C.; Siegrist, T.; Dabbagh, G.; Tully, J. C.; Walstedt, R. E. *J. Phys. Chem. Solids* **1992**, *53*, 1321–1332.

0897-4756/93/2805-0720$04.00/0

Benzonitrile (Fluka AG) was distilled from P_2O_5 under reduced pressure and stored under an argon atmosphere. C_{60} (Texas Fullerenes and Strem Chemicals, Inc.) was purified according to literature methods by extraction from carbon soot with toluene followed by separation from higher fullerenes on an alumina column with hexane chosen as the eluant.[17] Rubidium (99+%, courtesy of J. E. Schirber, Sandia National Laboratories) was used without further purification. All reaction glassware was assembled in an argon-filled drybox and reactions carried out on a vacuum/argon manifold due to the highly flammable nature of rubidium and rubidium doped C_{60}.

Solution Synthesis of RbC_{60}. In an argon drybox, C_{60} and elemental rubidium were combined in a 1:1 ratio in a Schlenk bottle. This reaction flask was transferred to a vacuum/argon manifold, and 30 mL of freshly distilled toluene was added via syringe. The reaction was allowed to reflux (111 °C) overnight under an argon atmosphere. The precipitated reaction product was collected by use of a Schlenk-type filter and dried under a vacuum of $\sim 10^{-2}$ Torr for 1 h.

Solution Synthesis of Rb_3C_{60}. In an argon drybox, C_{60} and elemental rubidium were combined in a 3.9:1 ratio in a Schlenk bottle. A slight excess of rubidium was found to be useful in preparing samples with high superconducting shielding fractions. This reaction flask was transferred to a vacuum/argon manifold. Freshly distilled toluene (27 mL) and benzonitrile (3 mL) were added via syringe. The reaction was allowed to reflux 2 h under an argon atmosphere. The black, precipitated reaction product was collected by use of a Schlenk-type filter and dried under a vacuum of $\sim 10^{-2}$ Torr for 2 h.

Vapor Synthesis of RbC_{60}. RbC_{60}, prepared by vapor-phase synthesis, was used as a calibration standard for X-ray powder diffraction and ESR. In an argon drybox, elemental rubidium and C_{60} were combined in a 1:1 ratio in a 6-mm quartz reaction tube. This reaction tube was transferred to a vacuum/argon manifold and evacuated to an argon pressure of $\sim 10^{-2}$ Torr. The tube was flame sealed and heated at 200 °C for 14 days.

Vapor Synthesis of Rb_3C_{60}. Rb_3C_{60}, prepared by vapor-phase synthesis, was used as a calibration standard for X-ray powder diffraction, ESR, and susceptibility measurements. In an argon drybox, elemental rubidium and C_{60} were combined in a 3:1 ratio in a 6-mm quartz reaction tube. This reaction tube was transferred to a vacuum/argon manifold and evacuated to an argon pressure of $\sim 10^{-2}$ Torr. The tube was flame sealed and heated at 200 °C for 8 days. The reaction mixture was then ground and pelletized in an argon drybox, resealed, and sintered at 250 °C for 8 days.

Chemical Analysis. As an independent check on the molar percentage calculation, one of the nonsuperconducting Rb_xC_{60} samples prepared from dry toluene was quantitatively analyzed with atomic absorption (AA) technique. On the basis of ESR analysis (see text), the sample contained 28 mol % of Rb_3C_{60} ($\Delta H = 14.4$ G) and 72 mol % of RbC_{60} (6.4 G). The bulk stoichiometry was $(Rb_3C_{60})_{0.28}(RbC_{60})_{0.72} = Rb_{1.56}C_{60}$. The results from AA analysis were Rb_nC_{60}, $n = 1.70, 1.76$, and $1.80 \pm 5\%$. The slightly higher AA rubidium analysis also indicated that there were small amounts ($\sim 5\%$) of other non-ESR active rubidium species such as RbOH and α-RbO_2 in the samples (see text).

X-ray Powder Diffraction. Samples of Rb_xC_{60} were sealed in glass capillaries and the X-ray powder diffraction patterns recorded at room temperature in a Debye–Scherrer film camera (radius 57.3 mm, Ni-filtered Cu $K\alpha$ radiation, $\lambda = 1.542$ Å). The samples were surrounded by 0.025-mm-thick Ni foil to suppress the fluorescence background. The width of the diffraction peaks was limited by the instrument geometry, indicating particles of >200-Å size.

Ac Susceptibility. Ac susceptibility measurements were performed with a Lake Shore Cryotronics 7221 ac susceptometer, operating at 1-G modulation field with a frequency of 111.1 Hz. The real (χ') and imaginary (χ'') components of the magnetic susceptibility were recorded between 4.5 and 50 K in temperature increments ranging from 0.1 (in the region of the superconducting transition) to 2.25 K (well above T_c). The superconducting shielding fractions were taken as the measured ac diamagnetic volume susceptibilities (χ' in SI units) at 5 K for zero-field cooling of the samples, relative to perfect shielding. In SI units, perfect shielding (100%) is represented by $\chi' = -1$. Sample volumes were based on the mass and theoretical density determined from reported X-ray structural studies. The instrument was factory calibrated to yield absolute susceptibilities, with calibration factors incorporated into the computer software used for instrument control and data acquisition. This calibration was checked with the use of a pure niobium metal cylinder with large length-to-diameter ratio (small demagnetization factor), which yielded a diamagnetic susceptibility of −0.98 on completion of a sharp superconducting transition with onset at 9.46 K. The susceptibilities of the fulleride samples were uncorrected for demagnetization because these are unknown quantities. The usual approximation used for powdered materials is to treat the particles as spheres with a demagnetization factor of $^1/_3$ (SI units). Application of this factor would lower the susceptibility by about 15% for shielding fractions of 50% ($\chi' = -0.5$) and by 3% for shielding fractions of 10% ($\chi' = -0.1$). Although not studied in detail, the Meissner fractions of some of our samples were found to be 14–28% of the shielding fractions.

ESR Spectroscopy. An IBM ER-200 ESR spectrometer (X-band, 9.4 GHz) with a TE_{102} rectangular cavity was used for ESR studies. Low-temperature measurements were carried out with either a 4111 VT liquid nitrogen variable temperature controller (300–100 K) or an Oxford Instruments liquid helium cryostat (300 to 4 K). The instrument was calibrated with a strong pitch ($g = 2.0028$). A locally developed computer program was used to fit first-derivative ESR spectra to a linear superposition of Lorentzian derivatives.[18] Because of the cubic symmetry of the ESR-active products, no corrections for g-value anisotropy were applied.

Results and Discussion

Solution Preparation of Rb_3C_{60}. In the original report of the solution phase synthesis of "Rb_xC_{60}", a 7% shielding fraction was determined at 5 K.[15] This preparation was carried out with a large (about 60-fold) excess of rubidium in reagent-grade toluene. In an attempt to increase the fraction of superconducting Rb_3C_{60}, experiments were performed in rigorously dried toluene with 3 equiv of elemental rubidium. The products obtained in these experiments showed little (less than 0.3%) or no superconductivity and were subsequently characterized as containing significant amounts of RbC_{60}.[40]

We found it important in producing Rb_3C_{60} to increase the polarity of the solvent to solubilize the C_{60}^- anion and prevent premature precipitation of C_{60} as RbC_{60}. The more polar benzonitrile was chosen as a solvent because of its miscibility in toluene and its ability to act as a "redox catalyst" in heterogeneous reactions,[19,20] transferring electrons from the molten alkali metal to the C_{60} molecules in solution. The reaction of C_{60} with 3 equiv of rubidium in neat benzonitrile resulted in a dark red solution characteristic of C_{60} anions,[21] but no precipitate formed. Subsequently, reactions in solvent mixtures of rigorously dried toluene and benzonitrile, with intermediate polarities, were attempted.

---

(17) Hare, J. P.; Kroto, H. W.; Taylor, R. *Chem. Phys. Lett.* **1991**, *177*, 394–398.

(18) Montgomery, L. K.; Geiser, U.; Wang, H. H.; Beno, M. A.; Schultz, A. J.; Kini, A. M.; Carlson, K. D.; Williams, J. M.; Whitworth, J. R.; Gates, B. D.; Cariss, C. S.; Pipan, C. M.; Donega, K. M.; Wenz, C.; Kwok, W. K.; Crabtree, G. W. *Synth. Met.* **1988**, *27*, A195.

(19) Swartz, J. E.; Stenzel, T. T. *J. Am. Chem. Soc.* **1984**, *106*, 2520–2524.

(20) Austin, E.; Alonso, R. A.; Rossi, R. A. *J. Org. Chem.* **1991**, *56*, 4486–4489.

(21) Heath, G. A.; McGrady, J. E.; Martin, R. L. *J. Chem. Soc., Chem. Commun.* **1992**, 1272–1274.

Scheme I. Stepwise Reduction of C_{60}

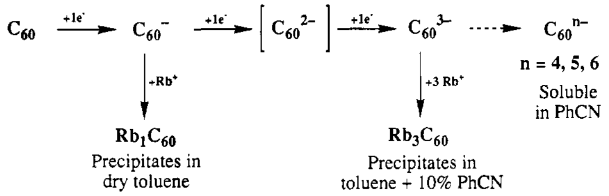

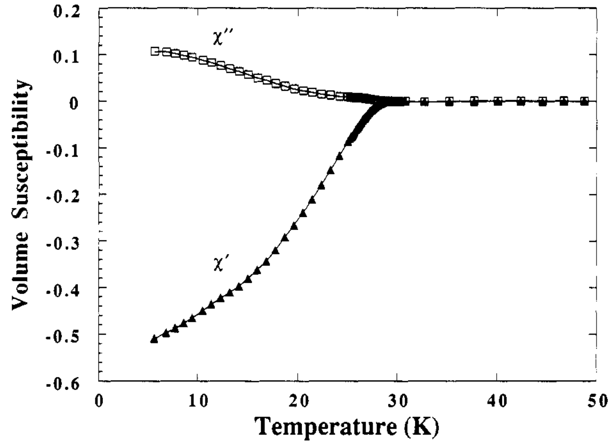

Figure 1. Variable-temperature ac magnetic susceptibility of Rb_3C_{60} prepared from a 9:1 toluene/benzonitrile solution phase synthesis (Table I, sample 5). χ' and χ'' represent the in-phase and out-of phase components, respectively.

Benzonitrile is known to react slowly with alkali metals forming a trimeric species,[22,23] but the short reaction times used in these experiments minimized the formation of this byproduct. The solubility of this trimer allowed it to be removed by filtration when the Rb_xC_{60} was collected. In some samples, traces of RbCN, also formed by the slow reaction of rubidium with benzonitrile, were detected by X-ray powder diffraction.

The proposed mechanism of Rb_3C_{60} formation is outlined in Scheme I. Our ESR study indicates that the reduction of C_{60} in solution initially gives rise to $C_{60}^{\bullet -}$ radical anions. When rigorously dried toluene is used as the reaction solvent, paramagnetic RbC_{60} precipitates and further reduction of the RbC_{60} solid by molten rubidium in the heterogeneous solvent mixture is expected to be slow, thereby resulting in low superconducting fractions. RbC_{60} is more soluble in a solvent system such as 10% benzonitrile in toluene, and the C_{60}^- anion remains in solution being further reduced to C_{60}^{3-}, before being precipitated as Rb_3C_{60}. Superconducting powders were collected from mixed solvents with benzonitrile concentrations between 5 and 20 vol %, with yields (based on initial C_{60} mass) generally near 75%. As the benzonitrile fraction increased, the yield decreased due to product dissolution and loss in the more polar filtrate.

The black precipitates obtained were vacuum dried, weighed, and sealed in capillary tubes. Superconducting shielding fractions were determined by use of ac susceptibility measurements. The variable-temperature susceptibility curve of the highest fraction sample is shown in Figure 1. The superconducting onset temperature is 29.0 ± 0.1 K with a shielding fraction of 51% at 5 K. The observed transition is much broader (ΔT 10–90% transition width = 13.9 K) than in materials obtained by vapor synthesis (ΔT 10–90% transition width = 9.2 K). This broadening may be due to the occurrence of very small particles with sizes comparable to or smaller than the London penetration depths, because one observes in Figure 1 that the diagmagnetic susceptibility (χ') does not reach full saturation even at 5 K (see subsequent discussion of penetration depths).

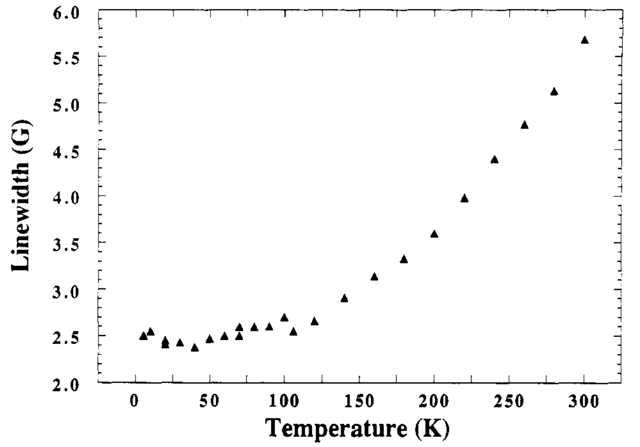

Figure 2. Variable-temperature ESR peak-to-peak line width of RbC_{60} prepared from solution-phase synthesis.

X-ray Powder Diffraction. X-ray powder diffraction was used to identify the various phases obtained by solution-phase synthesis. As expected, samples with higher shielding fractions were found to be richer in the Rb_3C_{60} phase. Samples prepared from solution with lower shielding fractions contained traces of RbOH, $RbOH{\cdot}H_2O$, and α-RbO_2. These products are produced by the reaction of elemental rubidium with trace amounts of water or oxygen. In the higher fraction samples, the above impurities were absent, but small amounts of RbCN were observed, which is formed by the decomposition of benzonitrile in the presence of rubidium.

ESR Characterization. The room-temperature ESR signal of RbC_{60}, prepared from solution, was analyzed by use of a locally developed least-squares line-shape analysis program.[18] The data were fit to a single Lorentzian line, with an agreement factor ($100\% \cdot \Sigma|\text{calc} - \text{obs}|/\Sigma|\text{obs}|$) of 3.8%, indicating a good fit. Since minor paramagnetic impurities can easily be observed from ESR line-shape analysis, we concluded that the sample contained only one ESR-active component. The ESR spectrum showed a peak-to-peak line width at 300 K of 5.7 G. The *g* value of 2.0006 is slightly larger than the values (1.999–2.0006) previously reported for the C_{60}^- monoanion in solution.[24–26]

Variable-temperature ESR measurements were also performed and the resulting peak-to-peak line widths were plotted against temperature in Figure 2. The line width decreased monotonically with temperature from 5.7 G at 300 K to 2.5 G at 100 K. Below 100 K, the line width was nearly temperature independent. This behavior was similar to that reported for a frozen solution of electro-

---

(22) Schlenk, W.; Bergmann, E. *Justus Liebigs Ann. Chem.* **1928**, *463*, 1–322.

(23) Kraus, G. A. *J. Am. Chem. Soc.* **1923**, *45*, 775.

(24) Kukolich, S. G.; Huffman, D. R. *Chem. Phys. Lett.* **1991**, *182*, 263–265.

(25) Allemand, P.; Srdanov, G.; Koch, A.; Khemani, K.; Wudl, F.; Rubin, Y.; Diederich, F.; Alvarez, M. M.; Anz, S. J.; Whetten, R. L. *J. Am. Chem. Soc.* **1991**, *113*, 2780–2781.

(26) Kato, T.; Kodama, T.; Oyama, M.; Okazaki, S.; Shida, T.; Nakagawa, T.; Matsui, Y.; Suzuki, S.; Shiromaru, H.; Yamauchi, K.; Achiba, Y. *Chem. Phys. Lett.* **1991**, *186*, 35–39.

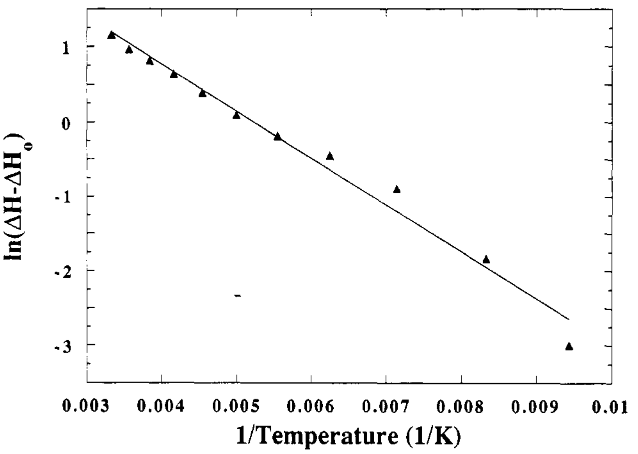

Figure 3. Plot of $\ln(\Delta H_T - \Delta H_0)$ versus $1/T$ of RbC_{60} prepared from solution. The equation used for the linear fit is: $\ln(\Delta H_T - 2.5) = 3.29 - 628/T$.

chemically generated C_{60}^- anions.[27,28] The reported C_{60}^{2-} dianion yields a distinct triplet ESR spectrum,[27-29] which was not observed in our RbC_{60} samples. The temperature dependence of the line width of the C_{60}^- monoanion samples was rationalized as a splitting of the triply degenerate t_{1u} orbitals of the parent C_{60} molecule due to a symmetry reduction.[26,28] The splitting was such that the doubly degenerate orbitals lie below the nondegenerate one. Assuming that the splitting is small, the two available electronic states of the monoanion would allow a thermal averaging, and the line-width behavior can be described with a thermally activated process as indicated in the following equation:

$$\ln(\Delta H_T - \Delta H_0) = A - E/kT$$

where ΔH_T is the ESR peak-to-peak line width at temperature T and ΔH_0 is the constant ESR line width at low temperature. The increase of the ESR line width with increasing temperature is associated with an activation energy, E. To check the validity of this argument for the RbC_{60} powder, the data above 100 K were fit to eq 1 with $\Delta H_0 = 2.5$ G, and the results plotted in Figure 3. The linear relationship observed suggests such that the above model is applicable, and the fitted activation energy is 0.063 eV. This is comparable to that observed for the C_{60}^- monoanion in frozen solvents, with activation energies ranging from 0.036 to 0.065 eV, depending on the organic solvent.[27]

The inverse of the ESR spin susceptibility for RbC_{60} is plotted versus temperature in Figure 4. The data scatter slightly below 20 K, but in general, Curie–Weiss behavior is observed. This result demonstrates that RbC_{60} is a paramagnetic species with localized spins, indicating semiconducting electrical properties. The large negative Weiss constant (~−450 K) suggests that the spins are coupled antiferromagnetically.

To characterize the ESR properties of the superconducting powder prepared by the solution phase technique, a Rb_3C_{60} sample was first prepared by the conventional vapor-phase method (vide supra) which showed a nearly

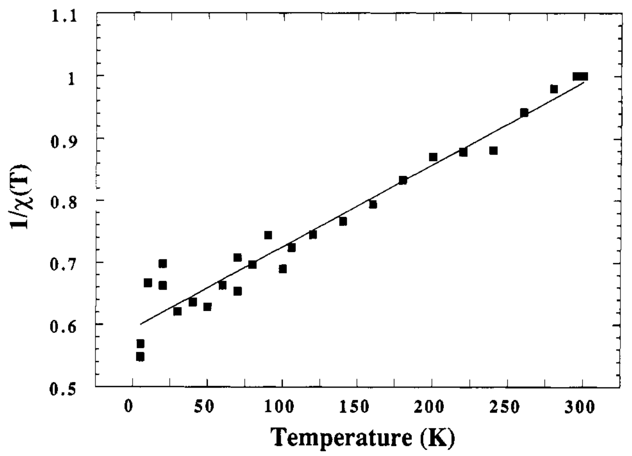

Figure 4. Inverse ESR spin susceptibility of RbC_{60} prepared from solution versus temperature.

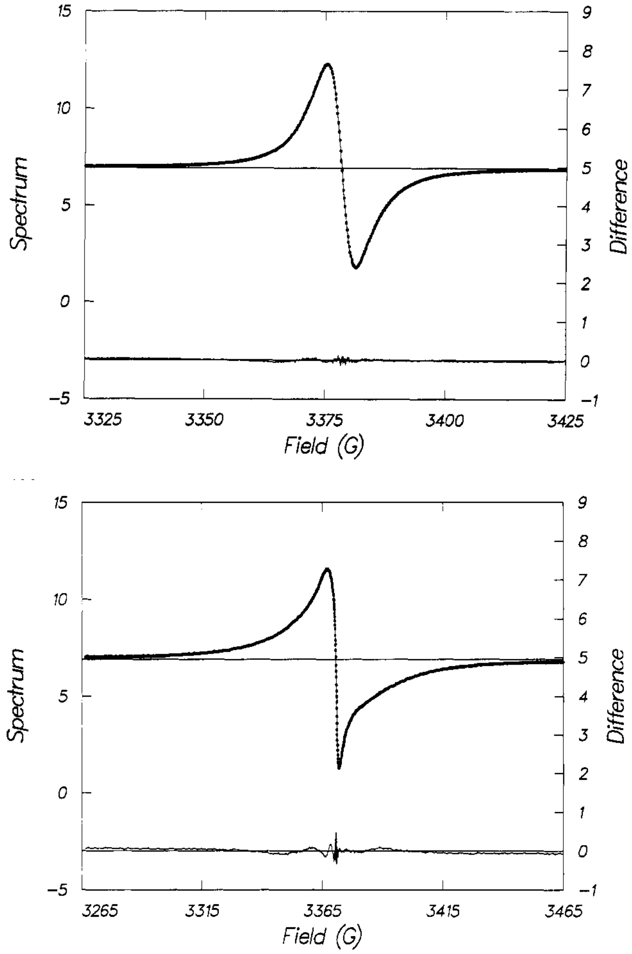

Figure 5. (a, top) ESR spectrum (circles) of a vapor phase synthesized Rb_3C_{60}. The calculated ESR spectrum with two components (see text) is shown with a solid line. (b, bottom) ESR spectrum (circles) of sample 4 (Table I) with calculated ESR spectrum (line) assuming three Lorentzian components. The difference between the original and calculated spectra is also plotted.

100% superconducting shielding fraction (without correction for demagnetization) and an onset T_c of 29.4 K. The ESR spectrum at 300 K showed two components (Figure 5a), a 12.7-G line (Rb_3C_{60}) and a 6.3-G line (RbC_{60}). By use of the previously analyzed RbC_{60} sample as a calibration standard for the paramagnetic components, this "high-fraction" sample was calculated to contain a 93:7 molar ratio of Rb_3C_{60} to RbC_{60}. Thus, even in high-

---

(27) Dubois, D.; Jones, M. T.; Kadish, K. M. *Mat. Res. Soc. Symp. Proc.* **1992**, *247*, 345–350.

(28) Dubois, D.; Jones, T. M.; Kadish, K. M. *J. Am. Chem. Soc.* **1992**, *114*, 6446–6451.

(29) Dubois, D.; Kadish, K. M.; Flanagan, S.; Haufler, R. E.; Chibante, L. P. F.; Wilson, L. J. *J. Am. Chem. Soc.* **1991**, *113*, 4364–4366.

Table I. ESR Line-Shape Analysis[a] and Superconductivity of the Rb_xC_{60} Synthesized from Solution-Phase Technique[b]

	sample 1		sample 2		sample 3		sample 4		sample 5	
	molar %	line width (G)	molar %	line width (G)	molar %	line width (G)	molar %	line width (G)	molar %	line width (G)
Rb_1C_{60}	28	7.9	23	5.3	23	8	8	6.0	4	8.8
Rb_3C_{60}	70	23.7	76	22.4	77	27	91	25.0	96	32.1
minor phase (see text)	2	2.6	1	1.8	0[c]	none	1	1.8	0[c]	none
R factor,[d] %	1.8		3.1		3.5		3.1		5.8	
superconducting shielding,[e] %	10		23		25		40		51	

[a] All analyses are based on ESR spectra recorded at 300 K. [b] All samples are prepared from rigorously dried toluene with 10% (volume) benzonitrile. [c] No detectable Rb_2C_{60} in the sample. [d] *R* factor % = $100\% \cdot \Sigma|\mathrm{calc} - \mathrm{obs}|/\Sigma|\mathrm{obs}|$. [e] Shielding fraction determined at 5 K with ac susceptibility measurements.

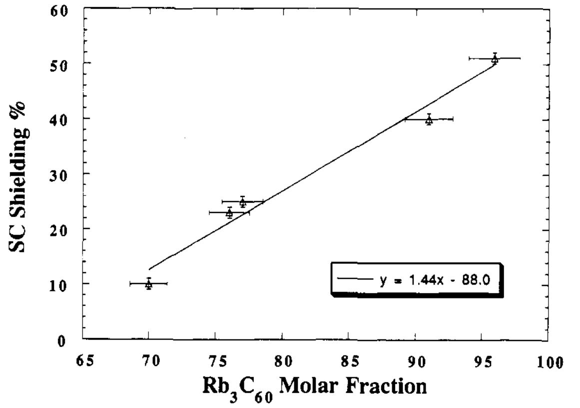

Figure 6. Superconducting shielding fraction of five different samples of Rb_xC_{60} (from Table I) prepared from solution synthesis in toluene/10% benzonitrile are plotted against the estimated Rb_3C_{60} molar percentage based on ESR line-shape analysis.

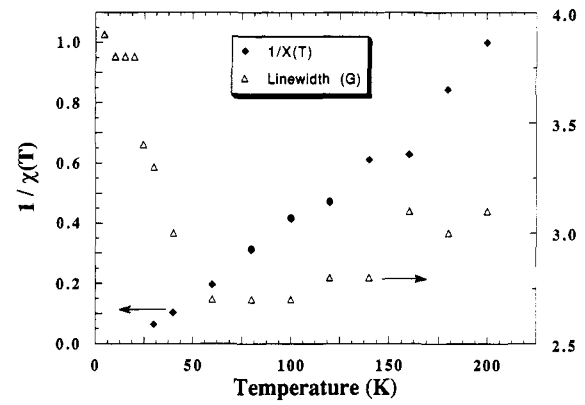

Figure 7. ESR peak-to-peak line width and the inverse of the spin susceptibility of a 23% RbC_{60} and 76% Rb_3C_{60} (sample 2) sample plotted against temperature.

fraction samples obtained from vapor phase synthesis, small amounts of RbC_{60} appear to be present.

The solution-phase superconducting samples were characterized by ESR analysis to contain two significant paramagnetic species. A typical spectrum is shown in Figure 5b. The major component has a line width of 22–32 G, with the smaller component having a width of 5–9 G. Occasionally, an unidentified impurity with a very sharp (1.8–2.6 G) line width was observed in less than 2% abundance. The 5-9-G line is attributed to RbC_{60} based on the previously described results herein for the material produced by direct solution synthesis of this compound. The broader 22–32 G line is assigned to the superconducting Rb_3C_{60}. Due to the broad solid state spectra, there is a large uncertainty associated with the *g* values (±0.002), which prohibits meaningful comparison among the *g* values of RbC_{60} and Rb_3C_{60}. The results of five such analyses are summarized in Table I. The range of shielding fractions is most likely a result of small differences in the starting Rb/C_{60} ratio and minor variations in the handling of these air sensitive materials. As shown in Figure 6, the molar fraction of Rb_3C_{60} calculated from the ESR studies is linearly correlated with the superconducting shielding fraction determined by use of ac susceptibility.

Samples prepared by this solution-based synthesis were observed to contain some residual solvent that could not be removed by drying at 100 °C under a reduced pressure of 10^{-4} Torr. Removal of solvent from solution prepared M_3C_{60} has previously been shown to be difficult, with heating to near 300 °C required to remove THF or NH_3.[16,39] Adhesion of phenyl groups to C_{60}^- anions has been observed previously,[30] suggesting that solvated benzonitrile would also be difficult to remove. This residual solvent is expected to broaden the ESR line width.[27]

The molar fractions of Rb_3C_{60} obtained by use of ESR are significantly higher than the superconducting shielding fractions obtained for the same samples. This likely originates in the smaller grain size expected to have been produced from solution as compared to the materials obtained from vapor-phase synthesis. Low values of the superconducting shielding fractions are obtained unless the grain size is much larger than the penetration depth.[16,31] The reported penetration depths for K_3C_{60} and Rb_3C_{60} are approximately 2400–4800 Å[32-34] while the grain size of M_3C_{60} prepared from vapor phase synthesis is on the order of 10 000 Å.[16,32] No direct measurements of the grain size in samples prepared from the solution-phase reactions are currently available.

The low-temperature ESR properties of sample 2 (76% Rb_3C_{60}, see Table I) were measured between 200 and 4 K. The spectra are dominated by the paramagnetic RbC_{60}, because of its narrower line width. Below 200 K, the ESR signals of the two components are similar in width, and thus the signal deconvolution procedures could not be applied because of high correlations. The dependence of the overall line width and inverse total spin susceptibility on temperature is shown in Figure 7. The total spin susceptibility between 200 and 30 K indicates a Curie–

---

(30) Krusic, P. J.; Wasserman, E.; Parkinson, B. A.; Malone, B.; Holler, E. R., Jr.; Keizer, P. N.; Morton, J. R.; Preston, K. F. *J. Am. Chem. Soc.* 1991, *113*, 6274–6275.

(31) Ramirez, A. P.; Kortan, A. R.; Rosseinsky, M. J.; Duclos, S. J.; Mujsce, A. M.; Haddon, R. C.; Murphy, D. W.; Makhija, A. V.; Zahurak, S. M.; Lyons, K. B. *Phys. Rev. Lett.* **1992**, *68*, 1058–1060.

(32) Uemura, Y. J.; Keren, A.; Le, L. P.; Luke, G. M.; Sternlieb, B. J.; Wu, W. D.; Brewer, J. H.; Whetten, R. L.; Huang, S. M.; Lin, S.; Kaner, R. B.; Diederich, F.; Donovan, S.; Grüner, G.; Holczer, K. *Nature* **1991**, *352*, 605–607.

(33) Holczer, K.; Klein, O.; Grüner, G.; Thompson, J. D.; Diederich, F.; Whetten, R. L. *Phys. Rev. Lett.* **1991**, *67*, 271–274.

(34) Sparn, G.; Thompson, J. D.; Huang, S.; Kaner, R. B.; Diederich, F.; Whetten, R. L.; Grüner, G.; Holczer, K. *Science* **1991**, *252*, 1829–1831.

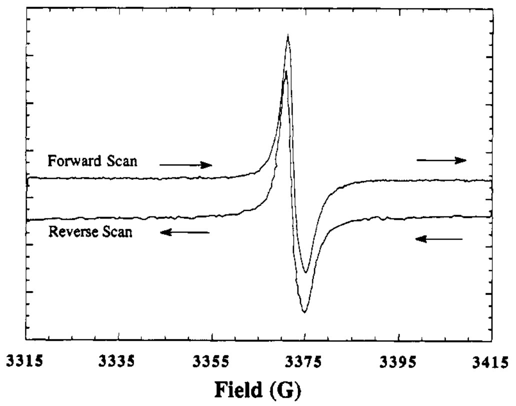

Figure 8. ESR spectrum of sample 2 (Table I) at 20 K. The vertical offset of the forward and reverse scans is caused by the magnetic hysteresis of the superconducting state and not by instrument settings.

Weiss behavior. Below 30 K, the intensity due to the paramagnetic RbC_{60} component is expected to continue to increase, while the contribution from Rb_3C_{60} is expected to vanish with the onset of superconductivity. A notable difference from single phase RbC_{60} is that the line width increases below 30 K. This is explained in terms of a paramagnetic species (RbC_{60}) suspended in a superconducting matrix (Rb_3C_{60}). Below T_c, the ESR line width of the paramagnetic species is broadened by the inhomogeneous magnetic field associated with the occurrence of a magnetic flux lattice in the superconducting species.[35,36]

Additional evidence for the coexistence of RbC_{60} and Rb_3C_{60} in the superconducting samples is shown in Figure 8 where the forward and reverse ESR scans of sample 2 at 20 K are illustrated without any change of the vertical offset. In the normal state, the forward and reverse scans are superimposable, but in the superconducting state a strong hysteresis loop due to the superconducting Rb_3C_{60} is clearly evident. The appearance of the hysteresis loop of a modulated microwave absorption is caused by the screening supercurrents which are synchronous with the modulated field, and which shift the phase by 180° as the direction of the sweeping is reversed.[37,38] The resonance with the 3.8 G line width observed below T_c is attributed to RbC_{60} alone.

Conclusions

A solution-phase method of preparing Rb_3C_{60} has been developed by use of a mixed solvent system (toluene/benzonitrile) that yields samples with relatively high (~50%) superconducting shielding fractions. The short reaction time (<2 h) makes this route attractive for large-scale synthesis. ESR line-shape analysis is a powerful tool that has been used to characterize the Rb_xC_{60} radical anion system. The major side product formed in the solution phase synthesis of Rb_3C_{60} has been identified as RbC_{60}, with a room temperature line width near 6 G. Rb_3C_{60} prepared by use of vapor phase reactions gives a line width of 12–14 G. The broader (22–32 G) line width observed in Rb_3C_{60} prepared from solution is attributed to traces of remnant solvent.

RbC_{60} can be prepared from a solution reaction using rigorously dried toluene as the solvent. This less polar solvent results in the precipitation of the C_{60}^- monoanion. The possibility that the sample has a bulk stoichiometry of RbC_{60} but is actually a mixture of Rb_3C_{60} and unreacted C_{60}, can be ruled out for several reasons: (1) The peak-to-peak ESR line width of Rb_3C_{60} is significantly broader (12–14 G) than that observed (5.1 G) for the RbC_{60} sample, and a line-shape analysis indicates that only one paramagnetic species is present. (2) The RbC_{60} sample shows no sign of superconductivity. (3) Unreacted, neutral C_{60} would be soluble in hot toluene solution and removed in the filtrate.

Traces of rubidium oxides and hydroxides have been identified in some products by use of X-ray powder diffraction techniques. The presence of these impurities is likely due to the reaction between rubidium and trace amounts of moisture during the chemical synthesis. Additional heat treatment near 250 °C of the solution phase synthesized samples does not increase the superconducting shielding fraction. This is likely due to the presence of chemical impurities. Our future efforts will involve the use of high-vacuum techniques, which will eliminate possible side reactions with water or oxygen, and potentially result in the rapid preparation of samples with even higher superconducting shielding fractions.

Acknowledgment. Work at Argonne National Laboratory is sponsored by the Office of Basic Energy Sciences, Division of Materials Sciences, U.S. Department of Energy, under Contracts W-31-109-ENG-38. M.W.L., J.D.D., and G.A.Y. are undergraduate research participants from Western Montana College, Dillon, MT, University of Wisconsin—Platteville, Platteville, WI, and The Pennsylvania State University, State College, PA, respectively, sponsored by the Division of Educational Programs. We would like to thank Dr. Harry Cohen for his helpful discussions. We are also grateful to Mr. Roland Lee and Professor J. E. Fischer (University of Pennsylvania) for performing X-ray analyses of some of our early samples.

---

(35) Puri, M.; Kevan, L. *Physica C* **1992**, *197*, 53–56.

(36) Shvachko, Y. N.; Koshta, A. A.; Romanyukha, A. A.; Naumov, S. V.; Ustinov, V. V. *Physica C* **1992**, *197*, 27–34.

(37) Atsarkin, V. A.; Demidov, V. V.; Noginova, N. E. *Superconductivity* **1992**, *5*, 301–309.

(38) Glarum, S. H.; Duclos, S. J.; Haddon, R. C. *J. Am. Chem. Soc.* **1992**, *114*, 1996–2001.

(39) Bausch, J. W.; Surya Prakash, G. K. Olah, G. A.; Tse, D. S.; Lorents, D. C.; Bae, Y. K.; Malhotra, R. *J. Am. Chem. Soc.* **1991**, *113*, 3205–3206.

(40) A series of MC_{60} (M = K, Rb, and Cs) compounds has recently been reported. Zhu, Q.; Zhou, O.; Bykovetz, N.; Fischer, J. E.; McGhie, A. R.; Romanow, W. J.; Lin, C. L.; Strongin, R. M.; Cichy, M. A.; Smith III, A. B. *Phys. Rev. B. Rapid Commun.*, submitted.